Macromolecules
ARTICLE

Macromolecules **2009**, *42*, 4511–4519 **4511**
DOI: 10.1021/ma9001897

One-Step Synthetic Route for Conducting Core−Shell Poly(styrene/pyrrole) Nanoparticles

Jung Min Lee, Dong Gyu Lee, Sun Jong Lee, and Jung Hyun Kim*

Department of Chemical and Biomolecular Engineering, Yonsei University, 134 Shinchon-Dong, Seodaemoon-Gu, Seoul 120-749, Republic of Korea

In Woo Cheong*

Department of Applied Chemistry, Kyungpook National University, 1370 Sankyuk-dong, Buk-gu, Daegu 702-701, Republic of Korea

Received January 28, 2009; Revised Manuscript Received May 22, 2009

ABSTRACT: Conducting core−shell poly(styrene/pyrrole) (poly(St/Py)) particles were successfully prepared by a one-step solution route in soap-free emulsion polymerization. Hydrogen peroxide (H_2O_2) and a trace of ferric chloride ($FeCl_3$) were used as an initiator couple to carry out Fe^{3+}-catalyzed oxidative polymerization. The average particle size of the particle was approximately 250 nm and its core−shell morphology (shell thickness ~20−30 nm) was proved with transmission electron microscopy. The SEM images after $CHCl_3$ dissolution supported a clear evidence of distinct core−shell morphology, and which was confirmed by DSC and TGA analyses. We proposed a growth mechanism for the formation of the core−shell poly(St/Py) particles based on the time-evolution morphology of the particle. The result was also corroborated by the time-evolution GPC, FT-IR and ζ-potential data. The surface compositions of the particles were examined by X-ray photoelectron spectroscopy (XPS). The doped particles showed a high conductivity in the dry state.

Introduction

Poly(pyrrole) (PPy) is not only an important component of conjugated polymers due to its usability in a wide range of applications, but also one of the most studied conducting polymers because it has a higher conductivity and better environmental stability in the conductive (oxidative) state than any other conducting polymers. PPy can be easily prepared by chemical oxidative[1] and electrochemical polymerization.[2] In a chemical oxidative polymerization, $(NH_4)_2S_2O_8$, H_2O_2, and many kinds of salts containing transition metal ions, e.g., $FeCl_3$ or $CuCl_2$, are generally used as oxidants. Particularly in the case of conventional chemical oxidative polymerization using $FeCl_3$ as an oxidant, a very large molar concentration of $FeCl_3$ (e.g., $FeCl_3$:pyrrole = 2.5:1) is often required to oxidize pyrrole monomers.[3] In addition, it should be removed from the final product to obtain the original electrical conductivity of the PPy; consequently, washing procedures such as washing after centrifugation,[4] dialysis[5] or extraction method with ethylenediaminetetraacetic acid (EDTA) solution are needed.[6] In this current work, however, only a trace amount of $FeCl_3$ was required to polymerize pyrrole monomers. Therefore, it is not necessary to remove $FeCl_3$ in the Fe^{3+}-catalyzed oxidative polymerization because only a catalytic amount of $FeCl_3$ was used.[7]

For the wide range application of PPy in various fields, it is important to improve its processability, conductivity, and environmental stability. Many researchers have focused on improving the processability of conducting polymers.[8−13] Often the solubilization of conductive polymers can be achieved through functionalization of the starting materials with a suitable side chain prior to polymerization.[14−16] These substituted PPys; however, possess a lower conductivity than the pristine PPys. Recently many other methods have been investigated in the preparation of soluble or swollen PPy[17−21] and dispersible fine powdered PPy[22−26] to improve their poor processability. For example, sterically stabilized PPy colloids can be easily synthesized in an aqueous media by chemically polymerizing pyrrole monomers in the presence of a suitable water-soluble polymer, such as methyl cellulose or poly(vinyl alcohol)[23,27] An alternate route for the preparation of colloidal conducting polymers involves coated particles with a thin layer of conjugated polymer to form conducting composites with a core−shell structure.[28−31] There have been numerous efforts to synthesize core−shell colloid materials with tailored structural, optical and surface properties, which are applicable to various fields, i.e., coatings, electronics, catalysis, separations, and diagnostics.[32−34] Its popularity is due to the expected improvement of polymer processability and the unique intrinsic properties in dispersed nanometer or micrometer-sized materials. If the conducting polymer shell-layer is continuous, it can lead to a relatively high conductivity in spite of the low conducting polymer loading. Yassar et al. reported that sulfonic and carboxylic acid coated poly(styrene) could be coated with PPy overlayer using $FeCl_3$.[25]

To the best of our knowledge, one-step solution route for the preparation of core−shell conducting polymer particles, i.e., poly(styrene/pyrrole) (poly(St/Py)), has never been reported. Usually, the core−shell conjugated polymer particles were prepared by multistep procedures using seed particles as a core material.[28−31,35,36] These techniques, however, have significant limitations of being both expensive and time-consuming due to the multistep procedures. Here, we proposed a facile method of

*Corresponding authors. (J.H.K.) Telephone: +82 2 2123 7633. Fax: +82 2 312 0305. E-mail: jayhkim@yonsei.ac.kr. (I.W.C.) Telephone: +82 53 950 7590. Fax: +82 53 950 6594. E-mail: inwoo@knu.ac.kr.

Published on Web 06/17/2009

preparing conducting polymer colloid particles with core−shell morphology using a one-step reaction.

Experimental Section

Materials. Styrene monomer (St, Junsei Chemical, Japan) was purchased and purified using an inhibitor remover column (Aldrich Co., Milwaukee, WI). The purified monomer was kept at −5 °C until used. Sodium *p*-styrene sulfonate (NaSS, Aldrich Co., Milwaukee, WI) was purchased and used as received. Pyrrole monomer (Py, Acros Organics) was refrigerated at −5 °C until used. Potassium persulfate (KPS, Junsei Chemical, Japan) and sodium bicarbonate ($NaHCO_3$, Aldrich, Milwaukee, WI) were analytical grades, and used without further purification. Anhydrous ferric chloride ($FeCl_3$, Kanto Chemical, Japan) and hydrogen peroxide (H_2O_2, DC Chemical, Korea) were used as a catalyst and an oxidant, respectively, without further purification. Double-distilled and deionized (DDI) water was used throughout the experiment.

Preparation of Core−Shell Poly(St/Py) Particles. Core−shell poly(St/Py) particles were synthesized in a 500 mL double-jacketed glass reactor, which was fitted with a reflux condenser, a nitrogen gas inlet, an ingredient inlet, and a Teflon-blade mechanical stirrer. The reaction temperature was 80 °C and maintained with a thermostat. The stirring rate was 400 rpm. The reaction procedure is as follows: NaSS (0.0017 mol, 0.36 g) and $NaHCO_3$ (0.0027 mol, 0.05 g) were dissolved in DDI water under N_2 atmosphere. H_2O_2 (0.441 mol, 15 g, 50% aqueous solution) was added to the reactant mixture solution. Styrene (0.115 mol, 12 g) and pyrrole (0.089 mol, 6 g) monomers were added to the mixture. After 0.5 h, KPS (0.002 mol, 0.012 g in 10 mL DDI water), $FeCl_3$ (0.0002 mol, 0.009 g in 10 mL DDI water) were added to the mixture and kept at the same reaction conditions for 5 h.

Characterization

Solid Content, Particle Size, and Stability Analysis (ζ-Potential) of Core−Shell Poly(St/Py) Particles. Solid content of the final latex particles, as determined by a gravimetrical method, was 6.25 wt %. The average particle size and particle size distribution were analyzed by capillary hydrodynamic fractionation (CHDF, CHDF-2000, Matec App. Sci.) at 20 °C. All samples were diluted with DDI water and redispersed with an Ultrasonic Processor VCX-500 sonicator (Watt, Sonics & Materials, Inc.) with a microtip at 20% power for 10 s. Colloidal stability of the core−shell poly(St/Py) particles was confirmed by ζ-potential analysis (Zeta-Sizer 3000 HSA, Malvern, U.K.).

Molecular Weight and Molecular Weight Distribution of the Core−Shell Poly(St/Py) Particles. Molecular weight and molecular weight distribution of the core−shell poly(St/Py) particles were obtained using a gel permeation chromatography (GPC, Waters Co.) equipped with a series of Waters columns (HR4, HR3, HR2, HR1), HPLC pump, RI detector, and data module at 40 °C. Molecular weights were determined from the refractive index data, which were analyzed with Waters Breeze System. Polystyrene standards and universal calibration was adapted to reduce measuring error. Eluent was tetrahydrofuran (THF) with a flow rate of 1.0 mL min^{-1}.

Morphology of Core−Shell Poly(St/Py) Particles. The surface and core−shell morphologies of poly(St/Py) particles were observed by using a transmission electron microscope (TEM; JEM-2000EXII, JEOL Co., Japan) and field-emission scanning electron microscope (FE-SEM; JSM-6500F, JEOL Co., Japan). The sample (30 mL; 0.1 wt %) deposited on a copper grid (200 mesh) was stained with the vapor of a 0.1 wt % RuO_4 aqueous solution at 40 °C and kept for 1 h in a fume cupboard. Afterward, the grid was dipped into a 0.4 wt % phosphotungstic acid aqueous solution, and the water was allowed to evaporate.

Thermal Property Analysis (DSC and TGA). A differential scanning calorimeter (DSC Q10, TA Instr.) was used to examine the glass transition temperature (T_g) of the core−shell poly(St/Py) particles prepared. The heating rate was 5 °C min^{-1} under an N_2 purge of 30 mL min^{-1}. The sample size was 10 mg in a sealed aluminum pan. DSC data were obtained from −50 to +250 °C.

Thermogravimetric analyzer (TGA Q50, TA Instruments) was used to examine the thermal degradation properties of the core−shell poly(St/Py) particles prepared. The sample weight was 10 mg. The experimental run was performed from 20 to 500 °C at a heating rate of 5 °C min^{-1} in a nitrogen atmosphere with a gas flow rate of 30 mL min^{-1}.

Growth of Core−Shell Poly(St/Py) Particles. Growth of core−shell poly(St/Py) particles was observed with a FE-SEM and a Fourier transform infrared spectroscopy (FT-IR; TENSOR 27, Bruker Optik GmbH, Germany) in a range of 400−4000 cm^{-1} at room temperature. For investigation of the time-evolution growth of the core−shell poly(St/Py) particles, all samples were taken at an appropriate time interval and exposed to a chloroform ($CHCl_3$) solution for 15 h to remove the core poly(St/NaSS) materials. Afterward, the samples were dried and monitored by FE-SEM.

Elementary Analysis of the Shell Surface of Core−Shell Poly(St/Py) Particles (XPS). Surface compositions of the PPy shell of the core−shell poly(St/Py) particles were examined by X-ray photoelectron spectroscopy (XPS, ESCALAB 220-IXL, VG Scientific Instrument). X-ray photoelectron spectroscopy (XPS) measurements have been carried out using Al Kα X-ray source (1486.6 eV). High resolutions scans with a good signal ratio have been obtained in C_{1s}, N_{1s}, O_{1s}, and S_{2p}. All the spectra have been recorded under ambient conditions.

Electrical Conductivity Measurement of Core−Shell Poly(St/Py) Particles. The electrical conductivity of core−shell poly(St/Py) particles was determined using a standard four-point probe technique (RT-70/RG-5 four point probe system, Napson Co., Japan) at room temperature. The powders (∼0.5 g) were pressed (∼5 ton) into pellets (3 mm thick, 12 mm diameter). The conventional four-point probe method (samples were pressed against four gold wires) was used to obtain the DC electrical conductivity of these pellets. Aging in inert atmosphere was performed by heating samples in dry nitrogen. The powders were treated as synthesized, then pressed into pellets for conductivity measurements. Sheet resistivity (in Ω/□) of the core−shell poly(St/Py) particles was measured and converted into electrical conductivity (S cm^{-1}).

Results and Discussion

Formation of the Core−Shell Poly(St/Py)Particles. Figure 1a shows a schematic for the formation of core−shell poly(St/Py) particles *via* Fe^{3+}-catalyzed oxidative polymerization and emulsifier-free emulsion polymerization. Before polymerization, the droplets of pyrrole and styrene monomers are dispersed in a continuous aqueous phase under vigorous agitation. Other water-soluble components, such as KPS, NaSS, and $FeCl_3$, as well as a small portion of styrene monomers (6.2 mM at 80 °C[37]) are dissolved in the aqueous phase. The oligomers of pyrrole are formed by oxidative polymerization in the presence of Fe^{3+} or KPS.[38] These oligomers form small aggregates (i.e., primary particles) due to hydrophobic interaction. At the same time, the oligomers of styrene/NaSS are formed by KPS *via* free-radical polymerization in the aqueous phase. As the chain

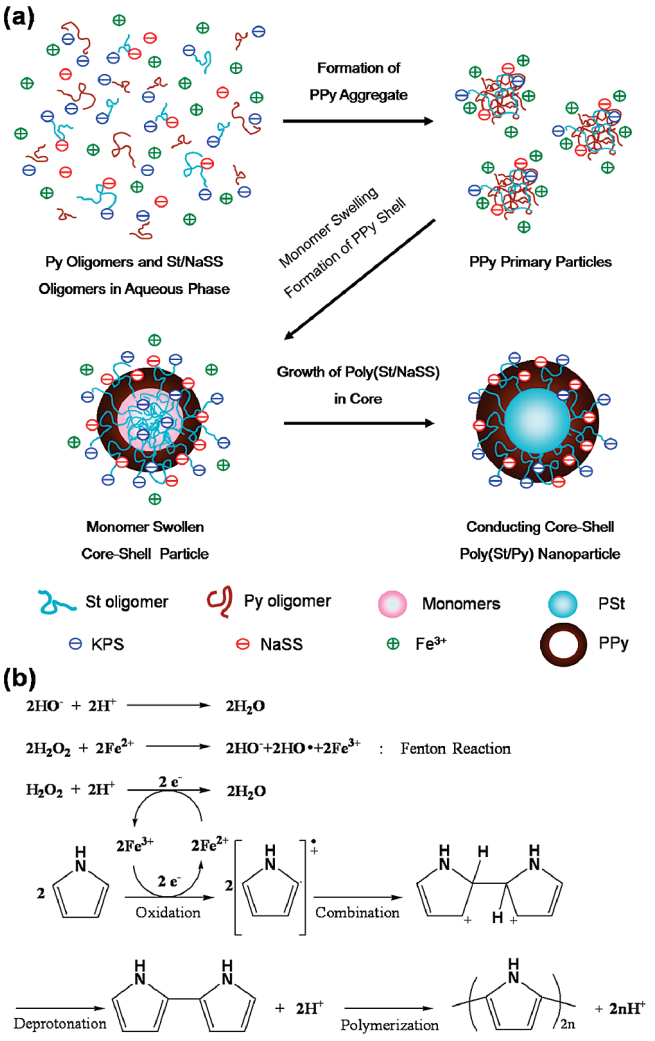

Figure 1. (a) Schematic illustration of the mechanism for the preparation of core−shell poly (St/Py) particles. (b) Detailed reaction mechanism of pyrrole monomers via Fe^{3+}-catalyzed oxidative polymerization.

length of the styrene/NaSS oligomer increases to *z*-mer ($^{\bullet}M_zSO_4^-$), they become surface active and enter into the primary particle of pyrrole oligomers. Anchoring of styrene/NaSS oligomers leads to the colloidal stabilization of the hydrophobic primary particles, since the hydrophilic moieties of SO_4^- (from KPS) and SO_3^- (from NaSS) are located the surface of the particle and the hydrophobic styrene units are located in the inner space of the particles. Styrene and pyrrole monomers can diffuse into the primary particles from the monomer droplets via continuous phase. Pyrrole monomer is predominantly polymerized at the surface of the primary particle, because the Fe^{3+} ions are enriched at the surface of the particle due to the ionic attraction between sulfate (SO_4^-) or sulfonate (SO_3^-) ions and Fe^{3+} ions. This provides an opportunity for a rapid oxidative polymerization of pyrrole at the water/particle interface. Consequently, PPy shell can be successfully formed at the surface of the particles.

In the beginning of the polymerization, the polymerization rate of styrene seems to be lower than that of pyrrole. In general, the oxidation reaction is faster than the thermal decomposition. Therefore, a portion of KPS can be used as an oxidant for the polymerization of pyrrole.[38] In addition, the standard reduction potential of KPS (+2.010 V) is higher than those of $FeCl_3$ and H_2O_2 (+0.771 and +1.776 V, respectively).[7] The PPy primary particles electro-statically stabilized can provide main polymerization loci to styrene monomers. As the polymerization of styrene monomers proceeds inside the particles, the core−shell poly(St/Py) particles are formed. The shell thickness increases by the oxidative polymerization of pyrrole with Fe^{3+} at the water/particle interface, in which three intermediate reaction steps are included: formation of a radical cation, radical combination, and deprotonation as illustrated in Figure 1b.

As seen in Figure 1b, the first step consists of the oxidation of the pyrrole monomer by Fe^{3+} ion and transformation into its radical cation. The second step involves the coupling of two radicals to produce the dihydro dimer dication that leads to a dimer after the loss of two protons and rearomatization in the third step. In the polymerization step, the dimer, which is more easily oxidized than the monomer, turns into its radical cation form by recyclable Fe^{3+} ions and undergoes a further coupling with a monomeric or oligomeric radical cation. During the oxidation of the pyrrole by Fe^{3+} ions, the Fe^{2+} ions formed by the oxidation reaction with pyrrole monomers can be reoxidized to Fe^{3+} ions by H_2O_2, which guarantees a high conversion of pyrrole monomers with only a trace of $FeCl_3$. In this process, water (H_2O) is formed as a byproduct. This recyclable reaction accompanies the Fenton reaction.[39] Hydroxide ions (OH^-) can be formed in aqueous solution by direct reaction of hydrogen peroxide (H_2O_2) with ferrous salt (Fe^{2+}). These hydroxide ions result in neutralization reaction, which also called a water forming reaction. In other words, hydroxide ions react with hydrogen ions (H^+), formed by deprotonation reaction of pyrrole dimer, to form water molecule. This indicates this synthetic method contains an environmentally friendly reaction system.

Particle Size and Molecular Weight of the Core−Shell Poly(St/Py) Particles. The representative SEM images of the core−shell poly(St/Py) particles are shown in Figure 2. The number average particle sizes (D_n) of the particles were about 250 and 420 nm, respectively, which is in good agreement with capillary hydrodynamic fractionation (CHDF) data (261.6 and 417.2 nm) in Figure 3. The CHDF data shows a bimodal peak of the core−shell poly(St/Py) particles. The bimodal distribution originates from the "existence" of surface active oligomers of styrene/NaSS. At the beginning of polymerization, the oligomers of pyrrole are instantly formed by KPS or Fe^{3+} to form aggregates due to their hydrophobicity. Until the oligomers of styrene/NaSS reach "*z*-mer", namely "surface active oligomer", the PPy aggregates would be unstable and keep coagulating. For this reason, the PPy aggregates before and after the formation of the styrene/NaSS oligomer would have different particle sizes. The anchoring of styrene/NaSS oligomers leads to the limited coagulation of the PPy aggregate. Therefore, the particle percentage at ca. 250 nm is predominant, while the particle percentage at ca. 420 nm seems negligible as shown in Figure 3.

Figure 4 shows the time-evolution M_w of the core−shell poly(St/Py) particles. Samples were taken at various intervals and analyzed after filtration. The obtained original PPy shells of the core−shell poly(St/Py) particles were insoluble in organic solvents; however, the poly(St/NaSS) core is soluble in THF, DMF and DMSO, etc. As shown in Figure 4 and Table 1, the poly(St/NaSS) core shows the M_w value of 41 899 g mol^{-1} at 300 min. While the M_w values of the styrene/NaSS oligomers in the core from 30 to 180 min actually increased from 384 to 878 g mol^{-1}, which is so small compared to the final M_w value. From this data, one can see that poly(St/NaSS) core could not be polymerized in the

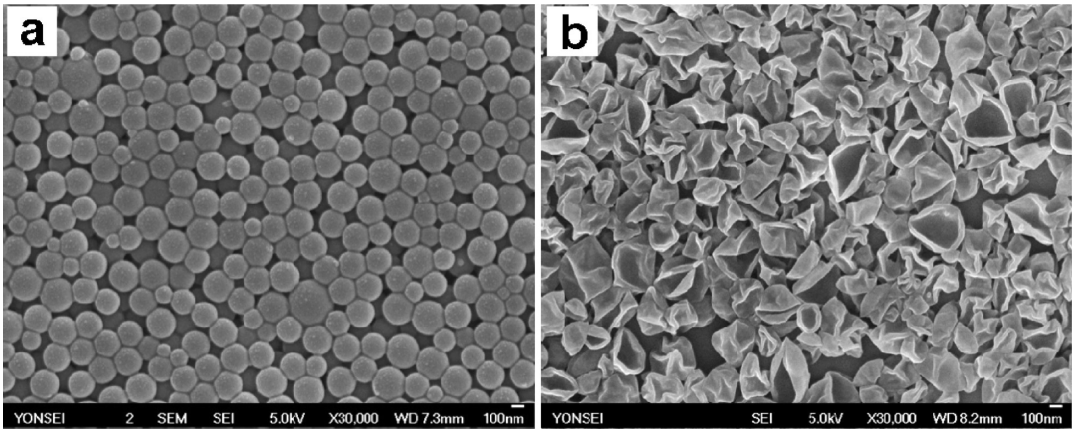

Figure 2. SEM images of (a) core−shell poly(St/Py) particles and (b) crumpled PPy shell layer of poly(St/Py) particles after $CHCl_3$ dissolution.

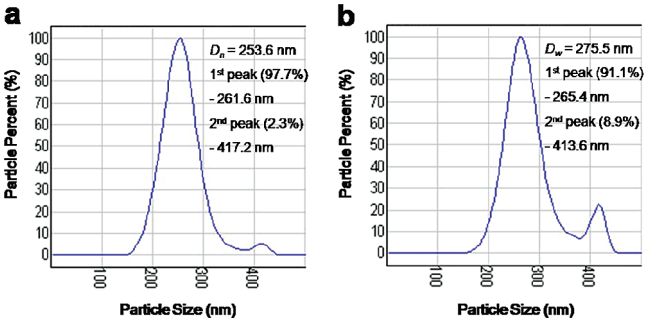

Figure 3. (a) Number average and (b) weight average particle size distributions of core−shell poly(St/Py) particles measured by using CHDF.

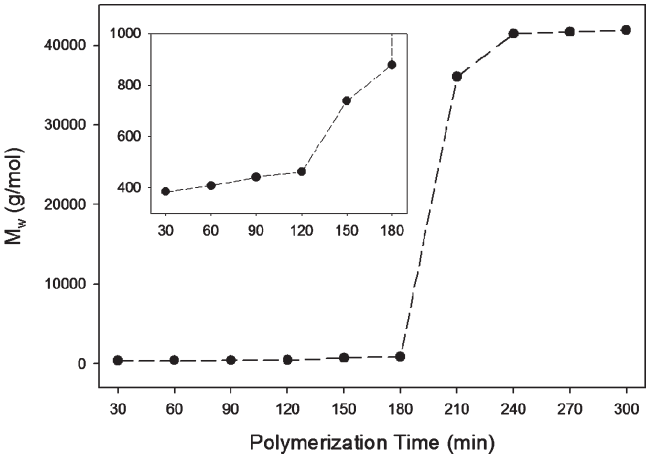

Figure 4. Time-evolution weight-average molecular weight data of the core−shell poly(St/Py) particles. The inset shows weight-average molecular weight data for the first 180 min.

early stage of the polymerization (i.e., until 180 min) due to the role of KPS as a oxidant for pyrrole monomers. This result is in accordance with the time-evolution SEM data as shown inFigure 7. This provides a strong evidence for the synthetic mechanism that the PPy shell was formed earlier than poly(St/NaSS) core. This result will be discussed in detail through time-evolution FT-IR measurements, as seen in Figure 8.

Morphology of the Core−Shell Poly(St/Py) Particles. To confirm core−shell morphology of the core−shell poly(St/Py) particles, they were exposed to a chloroform ($CHCl_3$) solution for 15−20 h to remove the poly(St/NaSS) core. As seen in Figure 2b, the image of crumpled PPy shells indicates the core−shell morphology of the resulting particles. Figure 5a shows the schematic and TEM micrograph for the compositions and inner structures of the individual core−shell poly(St/Py) particle. The particle size of the individual particle is approximately 150 nm. The thickness of the shell composed of PPy was 24 nm. As seen in the TEM images (Figure 5, parts b and c) with lower magnification showing more particles, all of the resultant spheres showed the core−shell structure with an average shell thickness of 20−30 nm for the PPy layer. As seen in Figure 5, one step reaction containing the two different monomers provides core−shell morphology and the outline of the poly(St/NaSS) core part is clearly shown. The contrast between the core and shell part is distinguishable, indicating that PPys are favorably located in the outer periphery (surface) of the particles. From this data, it can be concluded that the poly(St/Py) particles with the core−shell morphology, which was also corroborated by SEM data in Figure 2b, were successfully prepared by one-step reaction *via* the Fe^{3+}-catalyzed oxidative polymerization and emulsifier-free emulsion polymerization.

Thermal Properties of the Core−Shell Poly(St/Py) Particles. Figure 6 shows the thermal degradations of poly(St/NaSS), PPy, and core−shell poly(St/Py) particles. As seen in Figure 6, parts a and b, the initial decomposition temperatures of poly(St/NaSS) and PPy samples were about 395 and 120 °C, respectively. However, as seen in Figure 6c, the two onset points of decomposition of 395 and 120 °C were also observed in the core−shell poly(St/Py) sample. This result provides evidence that each composition of the core−shell poly(St/Py) particles, i.e., poly(St/NaSS) and PPy, maintained independent domains as core and shell.

Table 2 lists the values of T_g of pristine poly(St/NaSS), PPy, and core−shell poly(St/Py) particles prepared by using the Fe^{3+}-catalyzed oxidative polymerization and emulsifier-free emulsion polymerization. The glass transition of the poly(St/NaSS) (T_g = 108 °C) exhibited a typical sharp baseline shift while that of PPy (T_g = 70 °C) showed a broad temperature range. The T_g of the poly(St/NaSS) was about 38 °C higher than that of the homo PPy particle while two onset points of T_g (broad peak around 70−120 °C and sharp peak around 108 °C) were observed in the core−shell poly(St/Py) sample. This result was consistent with the TGA data. This can be explained by seeing that the absence of grafting reaction cites between the initiation of the vinyl groups of styrene monomers and the oxidative hydrogen abstraction of pyrrole monomers, originated from the different polymerization mechanism of each monomers, maintains

Table 1. Characteristics of the Core−Shell Poly(St/Py) Particles Prepared by Using Fe^{3+}-Catalyzed Oxidative Polymerization and Emulsifier-Free Emulsion Polymerization

sample	$\overline{D}_n$/nm	$\overline{D}_w$/nm	PDI[a]	$\overline{M}_n$/g mol^{-1}	$\overline{M}_w$/g mol^{-1}	PDI[b]	ζ-potential/mV
poly(St/Py) particles	253.6	275.5	1.09	20 527	41 899	2.04	−48.3

[a] PDI = $\overline{D}_w/\overline{D}_n$, $\overline{D}_w$ and $\overline{D}_n$ were measured by capillary hydrodynamic fractionation (CHDF) [b] PDI = $\overline{M}_w/\overline{M}_n$, $\overline{M}_w$, and $\overline{M}_n$ for poly(St/NaSS) cores were measured by gel permeation chromatography (GPC).

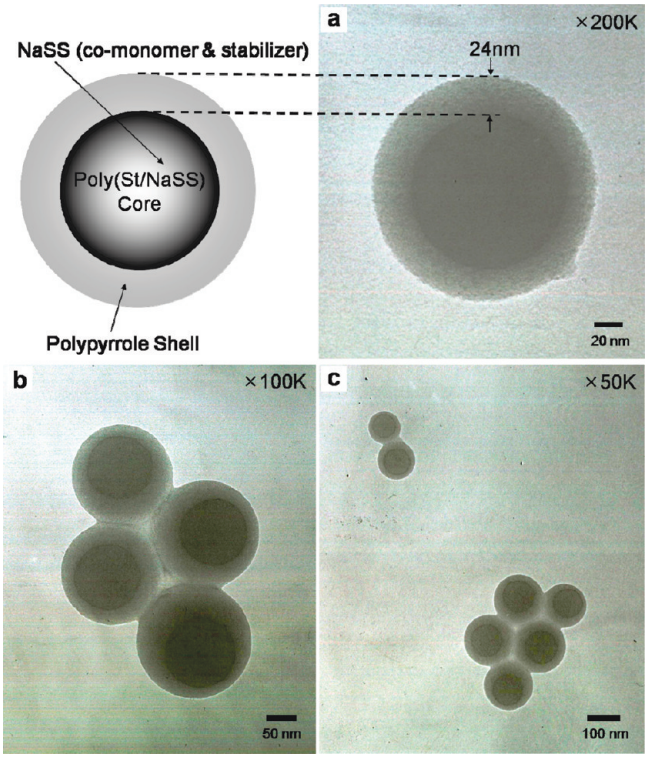

Figure 5. Representative TEM images of core−shell poly(St/Py) particle with a 24 nm thickness of PPy layer at (a) high magnification (×200K), (b) low magnification (×100K), and (c) lower magnification (×50K).

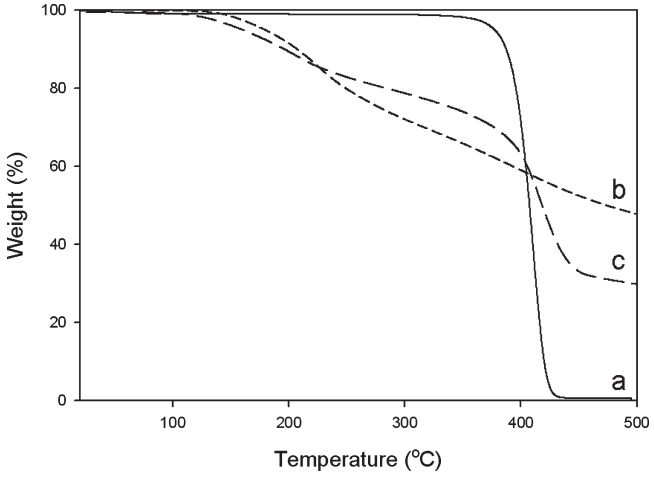

Figure 6. TGA curves of (a) pristine poly(St/NaSS), (b) pristine PPy, and (c) core−shell poly poly(St/Py) particles.

independent domains for each composition of the core−shell poly(St/Py) particles. This result was also confirmed by SEM and TEM analyses.

Synthetic Mechanism of the Core−Shell Poly(St/Py) Particles. Figure 7 shows the time-evolution SEM images of the core−shell poly(St/Py) particles before (a−e) and after (f−j) chloroform ($CHCl_3$) dissolution. In the investigation of the composition of the shell materials of the core−shell poly(St/Py) particles, the resulting core−shell poly(St/Py) particles in various polymerization time were exposed to a chloroform ($CHCl_3$) solution for 15 h to remove the core material, i.e., poly(St/NaSS). With the SEM images, one can see the formative process of the core−shell poly(St/Py) particles. A particle formation mechanism of the core−shell poly(St/Py) particles was explained above in Figures 1, 3, and 4. Above-mentioned elucidation was corroborated by the time-evolution SEM data, as seen in Figure 7. In the early stage of polymerization, i.e., 30 min, thin film was observed from the sample Figure 7a). After the chloroform ($CHCl_3$) dissolution, the thin film was observed as before (Figure 7f). This result indicates the thin film is distinctly composed of PPy, which is insoluble in $CHCl_3$ solution. At 90 min, before and after the $CHCl_3$ dissolution (Figure 7, parts b and g), we could find traces that the primary PPy aggregates had been formed in the aqueous phase. After 180 min of polymerization, a globular crumpled shell of PPy was formed. We can see that styrene monomers and oligomers were located in the core space of the core−shell poly(St/Py) particles before drying from Figure 7c and h. This globular crumpled shell of PPy remained unchanged after removal of the styrene monomers and oligomers in the core space (Figure 7h). As poly(St/NaSS) grew, the vacant spaces in the core of the core−shell poly(St/Py) particles were filled up completely (Figure 7c,d). After 300 min, spherical core−shell poly(St/Py) particles with a good stability were formed as seen in Figure 7e. These observations also supported the mechanism described above. This result can be corroborated by ζ-potential data as seen in Figure 8. Figure 8 shows that ζ-potential values of the core−shell poly(St/Py) particles decreased by 210 min during the polymerization and became constant thereafter. The negative ζ-potential values of the core−shell poly(St/Py) particles originates from the hydrophilic moieties of SO_4^- (from KPS) and SO_3^- (from NaSS). Throughout the polymerization, the concentration of NaSS copolymerized within styrene/NaSS oligomer chains was increasing continuously despite the tremendous radical loss that resulted from the oxidation reaction of pyrrole monomers by KPS. This result is due to the higher reactivity of NaSS than that of styrene monomer and the coexistence of NaSS and KPS in the aqueous phase. Consequently, lower ζ-potential values (−4.3 mV) of the core−shell poly(St/Py) particles were observed at the beginning of polymerization (10 min). As the polymerization proceeded, however, the concentration of NaSS in styrene/NaSS oligomers became higher. Therefore, higher ζ-potential values (−48.3 mV) of the core−shell poly(St/Py) particles were obtained. These higher ζ-potential values indicate the core−shell poly(St/Py) particles are very stable. From Figures 7 and 8, we can conclude that stable core−shell poly(St/Py) particles can be successfully prepared due to electrostatic stabilization of NaSS.

FT-IR spectra of the core−shell poly(St/Py) particles throughout the polymerization time are presented in Figure 9c−g. FT-IR spectra of pristine PPy and poly(St/NaSS) particles are also shown in Figure 9, parts a and b,

to compare with the peak position of the core−shell poly(St/Py) particles. As shown in Figure 9, parts a and b, FT-IR data for pristine PPy and poly(St/NaSS) particles were as follows.

•Pristine PPy particles (KBr, cm^{-1}): 3500−3300 (ν_{NH} stretching of pyrrole rings), 1640−1560 (ν_{NH} in-plane bending of pyrrole rings), 1350−1000 (ν_{CN} stretching of pyrrole rings).

•Pristine poly(St/NaSS) particles (KBr, cm^{-1}): 3100−3000 (ν_{CH} stretching of aromatic C−H groups), 3000−2900 (ν_{CH} stretching of aliphatic C−H groups), 2000−1650 ($\nu_{C=C}$

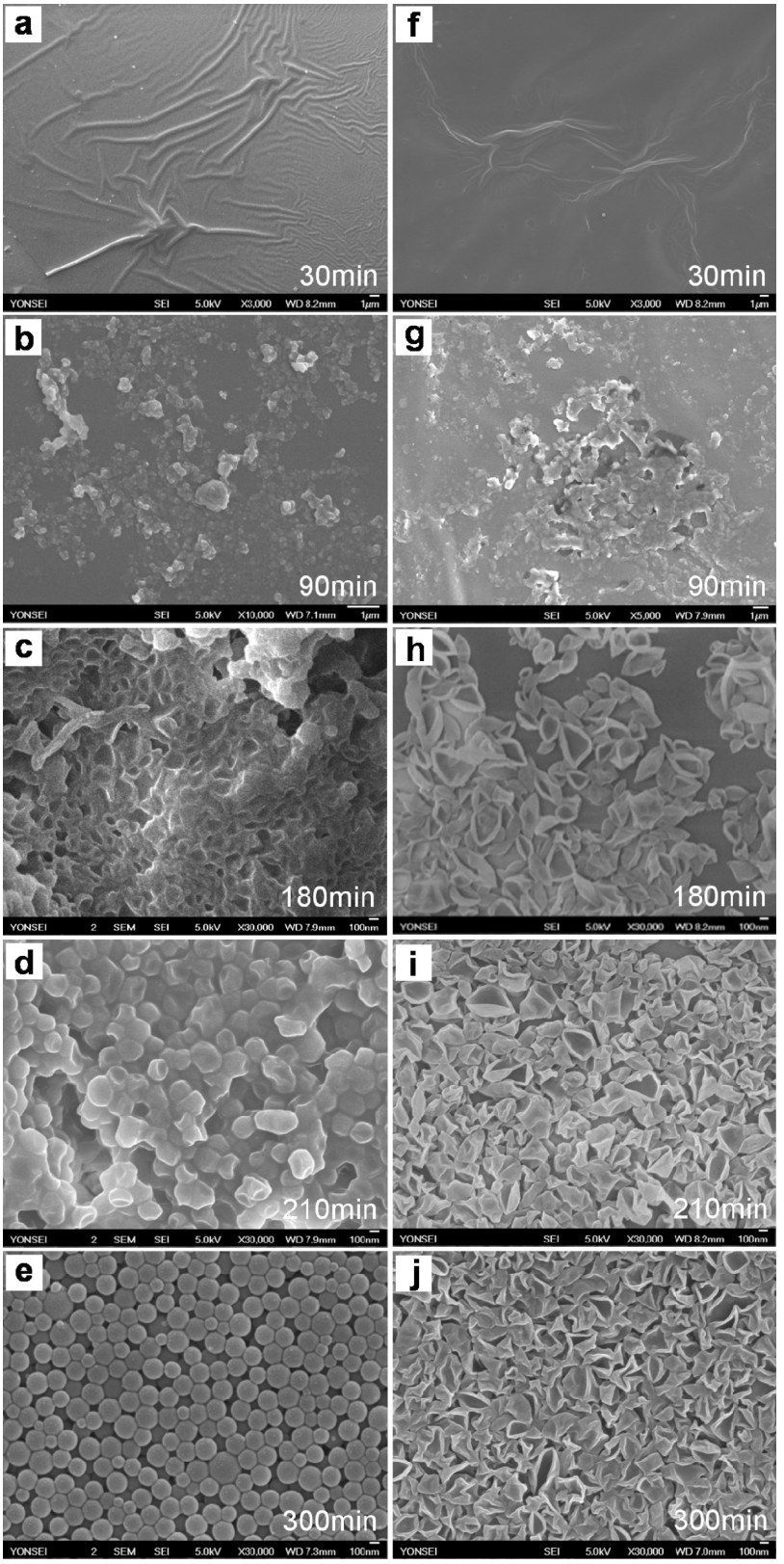

Figure 7. Time-evolution SEM images of core−shell poly(St/Py) particles before (a−e) and after (f−j) chloroform ($CHCl_3$) dissolution. The time in each SEM micrograph indicates the polymerization time.

Table 2. Thermal Properties of the Core−Shell Poly(St/Py) Particles

properties	sample code: pristine PPy homopolymer	pristine poly(St/NaSS) homopolymer	core−shell poly(St/Py) particles
glass transition temperature (T_g)	70−120 °C	108 °C	70−120 °C, 108 °C
initial thermal decomposition temperature (T_d)	120 °C	395 °C	120 °C, 395 °C

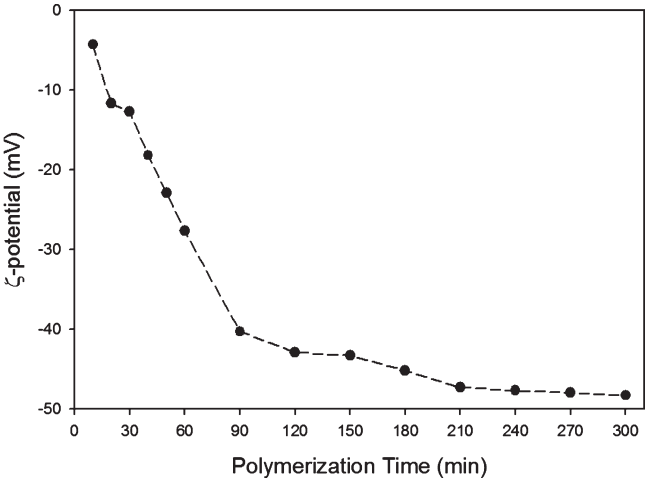

Figure 8. Time-evolution ζ-potential values of core−shell poly(St/Py) particles.

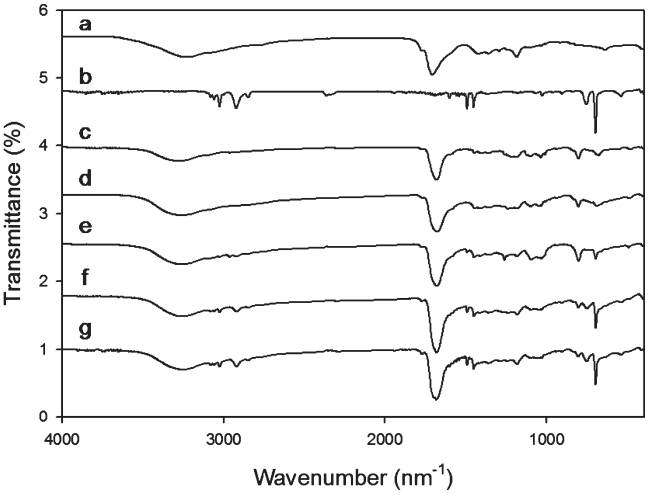

Figure 9. Time-evolution FT-IR spectra of (a) pristine PPy, (b) pristine poly(St/NaSS), and (c−g) core−shell poly poly(St/Py) particles. In order to investigate the reaction in each step of the particle formation, the intensity of CH stretching peaks of poly(St/NaSS) in the 3100−2900 cm^{-1} range were monitored every 30 min: (c) 30 min, (d) 90 min, (e) 180 min, (f) 210 min, and (g) 300 min.

overtone and combination bands of aromatic rings), 1600−1550 ($\nu_{C=C}$ stretching for aromatic rings), 1500−1450 ($\nu_{C=C}$ stretching for aromatic rings), 1300−1000 (ν_{CH} in-plane bending of aromatic rings), 780 and 700 (ν_{CH} out-of-plane bending of monosubstituted aromatic rings).

In order to confirm the reaction in each step of the particle formation, the intensity of CH stretching peaks of poly(St/NaSS) in the 3100−2900 cm^{-1} range were monitored every 30 min. The NH peak in the 3500−3300 cm^{-1} ranges was used as internal standard. As the reaction progressed, the intensity of aliphatic CH stretching peak increased from 180 min as seen in Figure 9e, indicating that the C=C double bonds of styrene monomers had reacted with propagating radicals and formed the C−C single bonds of poly(St/NaSS). This results were corroborated by the increased intensities of C=C overtone and combination bands of aromatic rings at 2000−1650 cm^{-1}, C=C stretching peaks of aromatic rings at 1600−1550 and 1500−1450 cm^{-1}, CH out-of-plane bending peaks of monosubstituted aromatic rings at 780 and 700 cm^{-1}. After completion of the polymerization reaction, the peak positions of the core−shell poly(St/Py) particles consistent with those of each pristine homopolymer confirmed that the independent domains for each composition of the core−shell poly(St/Py) particles still remained unchanged, as explained in Table 2 and Figure 6. In addition, it is confirmed that the rate of Fe^{3+}-catalyzed oxidative polymerization of pyrrole monomers is faster than the rate of free radical polymerization of styrene monomers from the time-evolution FT-IR data as shown in Figure 9c−g. This result was also verified by the time-evolution SEM data.

Surface Compositions of the Core−Shell Poly(St/Py) Particles. The surface compositions of the core−shell poly(St/Py) particles were examined by X-ray photoelectron spectroscopy (XPS). The N_{1s} XPS signal is a unique elemental marker for the PPy component and therefore was measured to confirm the elemental identity of the prepared PPy shell of the core−shell poly(St/Py) particles. Figure 10 depicts XPS survey spectra of the core−shell poly(St/Py)

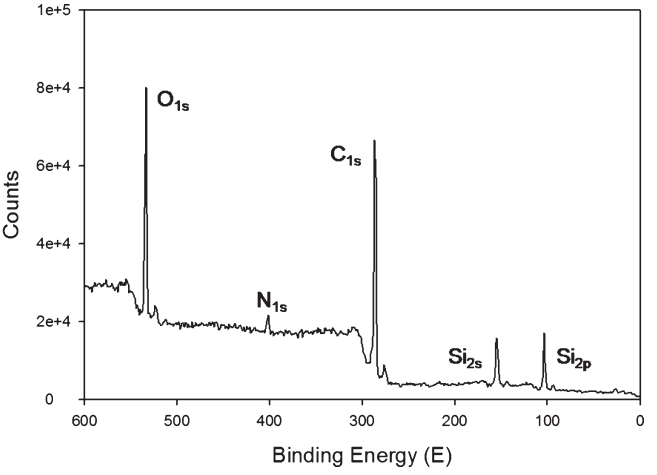

Figure 10. XPS survey spectra for core−shell poly(St/Py) particles on the cleaned glass substrate.

Table 3. The Electrical Conductivity Data for Core−Shell Poly(St/Py) Particles Fabricated by Using Fe^{3+}-Catalyzed Oxidative Polymerization

electrical property	values
sheet resistance [a] (Ω per square)	$3.01\times10^4 \pm 0.02$
specific resistance, ρ [b] (Ω·cm)	0.45
conductivity [c] ($S\cdot cm^{-1}$)	2.21

[a] Sheet resistances of the core−shell poly(St/Py) particles were determined using standard four-point probe techniques at 20 °C. [b] The thickness of the core−shell poly(St/Py) particles was 250 nm. [c] Conductivity = 1/specific resistance; The applied current and voltage were 10 μA and 100 mV, respectively.

Table 4. Electrical Conductivity Data for PPy Colloidal Particles Fabricated with Various Methods

research group	structure	synthetic method	conductivity (S/cm)	ref
our result	core−shell particles	Fe^{3+}-catalyzed oxidative polymerization via emulsifier-free emulsion polymerization	2.21	
Han et al.	core−shell particles	chemical oxidative polymerization via seeded suspension method	5.5×10^{-2}	46
Kim et al.	core−shell particles	chemical oxidative polymerization via seeded emulsion method	1.59	35
Omastova et al.	colloidal particles	chemical oxidative polymerization via emulsion method	5.5−9.9	45
Ishizu et al.	colloidal particles	chemical oxidative polymerization via emulsion method	1.0×10^{-5} to 1.0×10^{-1}	43
Armes et al.	colloidal particles	chemical oxidative polymerization via dispersion method	0.8−6.2	23
Qi et al.	colloidal particles	chemical oxidative polymerization via emulsion method	3.0	44

particles on the cleaned glass substrate. The Si_{2s}, Si_{2p}, O_{1s}, and N_{1s} signals due to the glass (SiO_2) substrate and PPy shell, respectively, were observed in the survey spectrum of the core−shell poly(St/Py) particles. The S_{2p} signal (167.1 or 168.5 eV)[40] of sulfonate or sulfate groups (SO_3^- or SO_4^-) was indiscernible due to the weak peak intensity and overlapping with the strong peak of Si_{2s} signal. This result arose from a relatively small amount of NaSS and KPS used compared with that of pyrrole monomer. The peak intensity of S_{2p} signal was negligible compared with that of N_{1s} signal of the PPy shell even though the sensitivity factor of sulfur (S) is higher than that of nitrogen (N).[41] From these results it can be concluded that the shell of the prepared core−shell poly(St/Py) particles are made of the PPy since N atoms are exclusively due to the PPy component.

Electrical Conductivity of the Core−Shell Poly(St/Py) Particles. Electrical resistance and conductivity data of the core−shell poly(St/Py) particles fabricated by using Fe^{3+}-catalyzed oxidative polymerization are given in Table 3. The conductivity of the core−shell poly(St/Py) particles was 2.21 $S \cdot cm^{-1}$. Doping level of the core−shell poly(St/Py) particles was 0.33. This value is the maximum doping level of PPy for Cl^- dopant.[42] Recently, electrical properties of conducting PPy colloidal and core−shell particles fabricated with various methods (i.e., dispersion, emulsion, and suspension, etc.) have been reported. We listed the values of electrical conductivity for PPy colloidal and core−shell particles prepared with different methods in Table 4. Conductivities of the PPy colloidal particles prepared by emulsion and dispersion methods were in the range of 10^{-5}−10^{-1} S/cm,[43] 3.0 S/cm,[44] 5.5−9.9 S/cm,[45] and 0.8−6.2 S/cm,[23] respectively, depending on the amount of dopant. In the case of PPy core−shell particles prepared by seeded suspension and emulsion methods, their conductivities were 5.5×10^{-2} S/cm[46] and 1.59 S/cm,[35] respectively. Comparing our results with published data, conductivity of the core−shell poly(St/Py) particles was comparable with the reported values of the various PPy colloidal and core−shell particles.

Conclusions

We demonstrated that the core−shell poly(St/Py) particles were successfully prepared by using Fe^{3+}-catalyzed oxidative polymerization with emulsifier-free emulsion polymerization in aqueous medium. The average particle sizes (D_n) of the particles were about 250 and 420 nm, which were confirmed from the analyses of SEM and CHDF. The prepared poly(St/Py) particles showed the core−shell morphology and maintained the independent domains (i.e., core and shell part) for each composition, poly(St/NaSS) and PPy, respectively. The growth mechanism for the particle formation of the core−shell poly(St/Py) particles was confirmed by the time-evolution SEM data, which is also corroborated by the time-evolution GPC, FT-IR and ζ-potential data. The resulting poly(St/Py) particles showed an excellent electrical conductivity (2.21 S/cm) due to the core−shell morphology. It is likely that the PPy is mainly located on the surface of the particles and this leads to a much higher electrical conductivity of the core−shell poly(St/Py) particles.

This new strategy is universal for the synthesis of many other conjugated materials with controlled morphology. This method can be effectively utilized to prepare the structured functional polymeric materials with various morphologies and inner structures for the bio- or chemical-sensor applications and electrical device fields.

Acknowledgment. This work was financially supported by the Korea Science and Engineering Foundation(KOSEF) grant funded by the Korea government(MOST) (Nos. R11-2007-050-02001-0 and R01-2007-000-10353-0). This work was supported by Nano R&D program through the Korea Science and Engineering Foundation funded by the Ministry of Education, Science and Technology (2008-02380). This work was also supported by the Seoul Research and Business Development Program (10816).

References and Notes

(1) Gardini, G. P. *Adv. Heterocycl. Chem.* **1973**, *15*, 67.
(2) Dall'Olio, A.; Dascola, G.; Varacca, V.; Bocchi, V. *C.R. Acad. Sci. Paris, Ser. C* **1968**, *267*, 433.
(3) Armes, S. P. *Synth. Met.* **1987**, *20*, 365.
(4) Mandal, T. K.; Mandal, B. M. *J. Polym. Sci., Part A: Polym. Chem.* **1999**, *37*, 3723.
(5) Giermanska-Kahn, J.; Schmitt, V.; Binks, B. P.; Leal-Calderon, F. *Langmuir* **2002**, *18*, 2515.
(6) Kumar, J.; Singh, R. K.; Rastogi, R. C.; Singh, R. *Mater. Chem. Phys.* **2007**, *101*, 336.
(7) Lee, S. J.; Lee, J. M.; Cheong, I. W.; Lee, H.; Kim, J. H. *J. Polym. Sci., Part A: Polym. Chem.* **2008**, *46*, 2097.
(8) Andreatta, A.; Cao, Y.; Chiang, J. C.; Heeger, A. J.; Smith, P. *Synth. Met.* **1988**, *26*, 383.
(9) Angelopoulos, M.; Asturias, G. E.; Ermer, S. P.; Ray, A.; Scherr, E. M.; Macdiarmid, A. G.; Akhtar, M.; Kiss, Z.; Epstein, A. J. *Mol. Cryst. Liq. Cryst.* **1988**, *160*, 151.
(10) De Chanterac, H.; Roduit, P.; Belhadj-Tahar, N.; Fourrier-Lamer, A.; Djigo, Y.; Aeiyach, S.; Lacaze, P. C. *Synth. Met.* **1992**, *52*, 183.
(11) Neoh, K. G.; Kang, E. T.; Tan, K. L. *J. Macromol. Sci., Pure Appl. Chem.* **1992**, *A29*, 401.
(12) Cao, Y.; Smith, P.; Heeger, A. J. *Synth. Met.* **1992**, *48*, 91.
(13) Lian, A.; Besner, S.; Dao, L. H. *Synth. Met.* **1995**, *74*, 21.
(14) Bergeron, J. Y.; Dao, L. H. *Macromolecules* **1992**, *25*, 3332.
(15) Ye, S.; Do, N. T.; Dao, L. H.; Vijh, A. K. *Synth. Met.* **1997**, *88*, 65.
(16) Dao, L. H.; Leclerc, M.; Guay, J.; Chevalier, J. W. *Synth. Met.* **1989**, *29*, E377.
(17) Jasne, S. J. 4 731 408, **1988**.

(18) Masuda, H.; Tanaka, S.; Kaeriyama, K. *J. Chem. Soc., Chem. Commun*. **1989**, 725.
(19) Takeishi, M.; H. K. a R. S. *Polym. Prepr. Jpn* **1991**, *40*, 2266.
(20) Stanke, D.; Hallensleben, M. L.; Toppare, L. *Synth. Met*. **1993**, *55*, 1108.
(21) Sato, H.; Nakama, K. Manufacture of electrically conductive, soluble pyrrole-3-carboxylic acid ester polymers. 92−180695−06206986, 19920708, **1994**.
(22) Bjorklund, R. B.; Liedberg, B. *J. Chem. Soc., Chem. Commun*. **1986**, 1293.
(23) Armes, S. P.; Miller, J. F.; Vincent, B. *J. Colloid Interface Sci*. **1987**, *118*, 410.
(24) Cawdery, N.; Obey, T. M.; Vincent, B. *J. Chem. Soc., Chem. Commun*. **1988**, 1189.
(25) Yassar, A.; Roncali, J.; Garnier, F. *Polym. Commun*. **1987**, *28*, 103.
(26) Aldissi, M.; Armes, S. P. *Prog. Org. Coat*. **1991**, *19*, 21.
(27) Armes, S. P.; Vincent, B. *J. Chem. Soc., Chem. Commun*. **1987**, 288.
(28) Lascelles, S. F.; Armes, S. P. *Adv. Mater*. **1995**, *7*, 864.
(29) Lascelles, S. F.; Armes, S. P.; Zhdan, P. A.; Greaves, S. J.; Brown, A. M.; Watts, J. F.; Leadley, S. R.; Luk, S. Y. *J. Mater. Chem*. **1997**, *7*, 1349.
(30) Bremer, L. G. B.; Verbong, M. W. C. G.; Webers, M. A. M.; van Doorn, M. A. M. M. *Synth. Met*. **1997**, *84*, 355.
(31) Lascelles, S. F.; Armes, S. P. *J. Mater. Chem*. **1997**, *7*, 1339.
(32) Wilcox, D. L., Sr., Berg, M., Bernat, T., Kellerman, D., Cochran, J. K., Jr., Eds. Hollow and Solid Spheres and Microspheres: Science and Technology Associated with their Fabrication and Application, Symposium held November 3−December 1, 1994, Boston, Massachusetts. *Mater. Res. Soc. Symp. Proc*. **1995**, *372*, 296.
(33) Davies, R.; Schurr, G. A.; Meenan, P.; Nelson, R. D.; Bergna, H. E.; Brevett, C. A. S.; Goldbaum, R. H. *Adv. Mater*. **1998**, *10*, 1264.
(34) Liz-Marzan, L. M.; Giersig, M.; Mulvaney, P. *Langmuir* **1996**, *12*, 4329.
(35) Kim, J. B.; Lim, S. T. *Polym. Bull*. **1996**, *37*, 321.
(36) Shin, J. S.; Lee, J. M.; Kim, J. H.; Suzuki, K.; Nomura, M.; Cheong, I. W. *Macromol. Res*. **2006**, *14*, 466.
(37) Lane, W. H. *Ind. Eng. Chem., Anal. Ed*. **1946**, *18*, 295.
(38) Kudoh, Y. *Synth. Met*. **1996**, *83*, 171.
(39) Tadolini, B.; Cabrini, L. *Mol. Cell. Biochem*. **1990**, *94*, 97.
(40) Zotti, G.; Zecchin, S.; Schiavon, G.; Louwet, F.; Groenendaal, L.; Crispin, X.; Osikowicz, W.; Salaneck, W.; Fahlman, M. *Macromolecules* **2003**, *36*, 3337.
(41) Ben Slimane, A.; Chehimi, M. M.; Vaulay, M.-J. *Colloid Polym. Sci*. **2004**, *282*, 314.
(42) Chandrasekhar, Prasanna *Conducting Polymers, Fundamentals and Applications*; Springer: Berlin, 1999; p 14.
(43) Ishizu, K.; Tanaka, H.; Saito, R.; Maruyama, T.; Yamamoto, T. *Polymer* **1996**, *37*, 863.
(44) Qi, Z.; Pickup, P. G. *Chem. Mater*. **1997**, *9*, 2934.
(45) Omastova, M.; Trchova, M.; Kovarova, J.; Stejskal, J. *Synth. Met*. **2003**, *138*, 447.
(46) Han, M.; Zhao, K.; Zhang, Y.; Chen, Z.; Chu, Y. *Colloids Surf., A* **2007**, *302*, 174.